TREE-RING RESEARCH, *Vol. 57(1), 2001, pp. 67–73*

AEGEAN TREE-RING SIGNATURE YEARS EXPLAINED

MALCOLM K. HUGHES

Laboratory of Tree-Ring Research
University of Arizona
Tucson, AZ 85721, USA

PETER IAN KUNIHOLM

Malcolm and Carolyn Wiener Laboratory for Aegean and Near Eastern Dendrochronology
B-48 Goldwin Smith Hall
Cornell University
Ithaca, NY 14853-3201, USA

JON K. EISCHEID

Cooperative Institute for Research in Environmental Science
University of Colorado
Boulder, CO 80309, USA

GREGG GARFIN

Laboratory of Tree-Ring Research
University of Arizona
Tucson, AZ 85721, USA

CAROL B. GRIGGS and **CHRISTINE LATINI**

Malcolm and Carolyn Wiener Laboratory for Aegean and Near Eastern Dendrochronology
B-48 Goldwin Smith Hall
Cornell University
Ithaca, NY 14853-3201, USA

ABSTRACT

As a long master tree-ring chronology for the region around the Aegean approaches completion, timbers from monuments and archaeological sites as far as 2,000 km apart, and as far back as 7000 BC, are being dated. The patterns used in this dating are characterized by signature years, in which trees at the majority of the sites have smaller or broader rings than in the previous year. We show that the signature years are consistently associated with specific, persistent, circulation anomalies that control the access of precipitation-bearing systems to the region in springtime. This explains the feasibility of dating wooden objects from widely dispersed sites, and opens the possibility of reconstructing aspects of the climate in which the wood grew.

Keywords: Aegean, Greece, Turkey, Italy, signature years, precipitational anomalies, circulation anomalies.

INTRODUCTION

Tree-ring dating has been used by workers at the Malcolm and Carolyn Wiener Laboratory for Aegean and Near Eastern Dendrochronology at Cornell University to date over 270 medieval and ancient sites (Kuniholm and Striker 1987; Kuniholm 1990, 1996; Kuniholm and Newton 1992;

Kuniholm *et al.* 1992, 1993a, 1993b, 1995). This has already had significant implications for the interpretation of many well-known archaeological sites, *e.g.* Herculaneum, Troy, Egyptian pyramids and coffins, and dozens of lesser-known sites. An indication of why this might be possible was predicted by a 1942 study of 67 tree-ring cores taken from living *Pinus nigra* Arn. on the north-central Anatolian plateau. The authors compared relative tree-ring widths with corresponding meteorological data for the years 1881–1892 and 1927–1938 (Gassner and Christiansen-Weniger 1942). Relatively small rings were noted in 1882, 1886, 1887, 1890, 1928, and 1935, and relatively large rings in 1881, 1930, and 1936 in a majority of cores, corresponding to less or more precipitation in those years. We have been able to test these findings with a greatly expanded set of tree-ring samples and much longer meteorological records.

TREE-RING MATERIALS

Only chronologies from living or recently-felled trees were used because those trees' exact locations are known. The period analyzed, the century of 1880–1979, was determined by availability of adequate meteorological data and the end-dates of the tree-ring chronologies. Twenty-three chronologies were selected, each constructed from trees from one genus, and most from one species, representing 6 genera and at least 10 tree species (Figure 1, Table 1). They were selected on the basis of the time period covered, level of replication, and strength of common (presumably climatic) signal shared by the individual trees at a site as indicated by percent variance captured by a simple response function (see below and Table 1). The chronologies come from sites with diverse ecological and geological conditions. Site climates range from the cool, wet winter and hot, dry summer climate typical of southern Greece, to the mild, very wet climate of the coastal mountains of northeastern Turkey.

The regional signal in each site chronology was optimized by using the ARSTAN program (Cook 1985). A curve was fit to each sample series of ring-widths tightly enough to remove century-scale variations, leaving decade and multi-decade

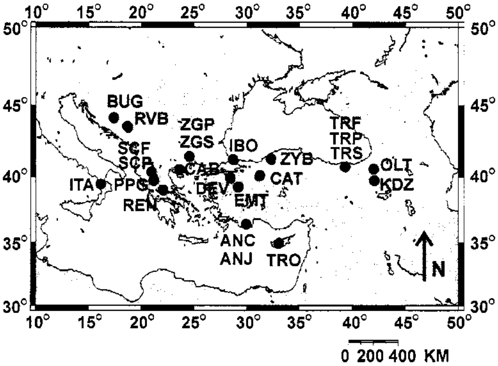

Figure 1. Locations of the 23 tree-ring chronologies referred to in this article. Some locations yielded two or more chronologies, each from a different tree species. The three-letter codes refer to the site names given in Table 1.

variations intact. Then the year-to-year non-climatic persistence that is seen in some samples as a high mean correlation between one year's ring-width and the next was removed using a technique known as prewhitening. The values for each year from all the samples at a site were then combined into an average series, the site chronology. This represents the variation common to the cores taken at this site, and is effectively a summary of much of the information the dendrochronologist uses when attempting to date a new sample against an existing chronology.

TESTING FOR CLIMATE SIGNAL

To test for a climate signal, we used a simple model of a climate/tree growth relationship and calculated response functions (Fritts *et al.* 1971). Monthly mean temperature and total monthly precipitation for the period of October from the year before growth through September of the growth year were used as predictors. Tree-ring width indices were predicted. Monthly station precipitation data were obtained from the US Department of Energy global precipitation database (Eischeid *et al.* 1991). All stations in the region shown in Figure 1 were considered as candidates for use. Missing data were estimated by multiplying the median ratio between the missing data station and its most highly correlated nearest neighbor by the nearest

Table 1. Chronology site details.

Code	Name	Lat. N	Long. E	Elev. (m)	Species	Response Function % var.	F	p
ITA	Mt. Pollino	39°26′	16°12′	1400–1500	*Pinus leukodermis*	30	3.1	.001
BUG	Bugojno	44°05′	17°25′	730–950	*Pinus nigra*	23	2.5	.013
RVB	Ravno Borje	43°25′	18°45′	800	*Pinus nigra*	35	5.9	.000
SCF	Scotida	40°20′	21°00′	1500	*Abies cephallonica*	35	5.9	.000
SCP	Scotida	40°20′	21°00′	1500	*Pinus nigra*	30	4.8	.000
PPG	Grevena	39°55′	21°10′	1600	*Pinus leukodermis*	33	6.9	.000
REN	Rendina	39°04′	21°58′	800	*Quercus* sp.	42	3.7	.035
CAB	Chalkidiki	40°34′	23°42′	600	*Quercus* sp.	37	2.4	.069
ZGP	Zagradeniye	41°25′	24°36′	1710	*Pinus nigra*	33	2.9	.013
ZGS	Zagradeniye	41°25′	24°36′	1710	*Picea abies*	42	3.1	.030
DEV	Devecikonak	39°50′	28°30′	550–950	*Quercus* sp.	47	2.7	.028
IBO	Istanbul	41°10′	28°50′	150	*Quercus* sp.	49	4.2	.004
EMT	Emet	39°20′	29°15′	1200	*Pinus nigra*	57	4.4	.000
ANC	Antalya	36°30′	30°00′	1800	*Cedrus libani*	26	2.5	.025
ANJ	Antalya	36°30′	30°00′	1800	*Juniperus* spp.	37	2.9	.008
CAT	Çatacık	40°00′	31°05′	1818	*Pinus nigra*	49	5.4	.000
ZYB	Zonguldak	41°10′	32°20′	1140–1340	*Quercus hartwissiana*	57	4.7	.001
TRO	Troodos	34°55′	32°55′	1600	*Pinus nigra*	39	4.2	.000
TRP	Torul	40°40′	39°20′	1300–1400	*Pinus sylvestris*	56	5.3	.000
TRF	Torul	40°40′	39°20′	1300–1400	*Abies nordmanniana*	33	3.05	.007
KDZ	Karınca Duzu	40°00′	42°00′	2700	*Pinus sylvestris*	43	4.8	.000
OLT	Oltu	40°35′	42°00′	2100	*Pinus sylvestris*	38	3.4	.004

neighbor precipitation. In addition to the quality control measures employed by Eischeid *et al.* (1991), each station was tested for inhomogeneity using Potter's t-test (Potter 1981). Station data were then interpolated to the location of the tree-ring samples, using an algorithm whereby precipitation values were weighted by the inverse of the squared distance between the station and the tree-ring site. The locations of the stations used in this interpolation are shown in Figure 2. Temperature values were weighted by the linear inverse of the distance between the tree-ring site and the meteorological station. These data were used in the calculation of response functions for each tree-ring site.

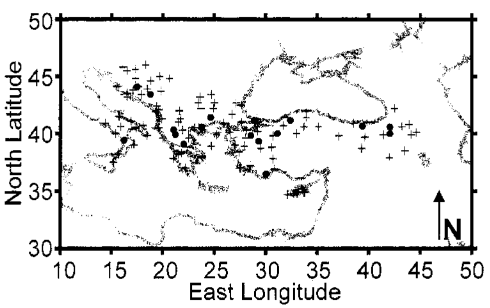

Figure 2. Location of the meteorological stations used in the response function analysis. The closed circles indicate the tree-ring sites, the plus signs the meteorological stations.

The most consistently significant relationship of tree-ring growth to climate data in the results of this test was the positive growth response to spring and early summer precipitation (Figure 3). This was particularly marked in May and June in the easternmost half of the study area, and in April in its center. The effect was weaker in Greece, although there was a tendency for negative responses to temperature in May and June, which, given a negative correlation between temperature and precipitation, reflects similar weather conditions to the eastern part of the region. Thus we defined the common climate signal for this region as the total April through June precipitation.

CLIMATE RESPONSE FUNCTIONS

SITES	TEMPERATURE												PRECIPITATION											
	O	N	D	J	F	M	A	M	J	J	A	S	O	N	D	J	F	M	A	M	J	J	A	S
ITA	**+**	−	**−**	−	**+**	−	+	−	**−**	−	+	−	**−**	−	+	+	−	−	−	−	+	−	−	+
BUG	+	+	−	**+**	+	+	**+**	−	**−**	**−**	−	**−**	+	−	−	+	−	+	+	+	−	**+**	−	**−**
RVB	−	+	−	+	**+**	+	**+**	**−**	**−**	**−**	−	−	**−**	**−**	+	−	**−**	−	**−**	**+**	+	+	+	−
SCF	**−**	**−**	**+**	+	−	+	**+**	**−**	**−**	**−**	−	−	+	+	**−**	**−**	+	**−**	**−**	+	**+**	−	+	−
SCP	+	+	−	+	−	**+**	+	**−**	**−**	**−**	−	−	+	+	−	**−**	−	**−**	+	**+**	+	**+**	−	−
PPG	−	**+**	**+**	**−**	+	**+**	**+**	−	**−**	**−**	**−**	**−**	−	−	+	−	**−**	**−**	**−**	+	**+**	+	−	**−**
REN	−	**+**	−	**−**	+	+	**−**	−	**−**	**+**	+	**−**	**−**	−	**+**	**+**	+	**+**	**+**	**+**	+	−	−	**−**
CAB	+	−	−	+	+	**−**	+	+	−	−	+	−	+	+	**−**	**−**	**+**	+	**−**	+	+	+	+	−
ZGP	−	+	+	+	−	**+**	+	−	−	−	**+**	+	−	−	+	−	+	**−**	**+**	−	+	+	−	−
ZGS	+	−	−	**−**	−	−	+	+	−	**+**	+	−	−	+	−	−	+	**−**	**+**	−	**−**	−	**−**	**−**
DEV	+	−	−	**+**	−	**+**	−	**−**	+	+	−	**−**	+	−	+	+	+	−	−	+	+	−	+	−
IBO	−	−	−	−	**−**	**+**	+	−	+	**+**	+	−	+	+	−	**+**	**+**	**+**	+	**+**	+	−	+	−
EMT	−	−	**+**	+	−	+	**+**	−	+	+	**−**	+	−	+	**+**	**+**	+	−	**+**	**+**	**+**	+	**+**	−
ANC	−	−	+	−	+	−	+	**+**	−	+	−	**+**	+	−	+	+	+	+	−	**+**	**+**	−	**+**	**+**
ANJ	+	−	−	−	+	−	−	−	+	−	+	**+**	+	−	**+**	+	−	+	+	**+**	+	**+**	+	**+**
CAT	−	+	**+**	−	**−**	+	**+**	+	+	**+**	**+**	+	−	+	+	**+**	−	−	**+**	**+**	**+**	+	+	+
ZYB	−	+	−	−	**−**	+	**+**	+	−	+	**+**	+	+	**−**	**+**	**+**	**−**	−	+	+	**+**	**+**	+	−
TRO	−	**−**	+	**+**	+	−	**+**	−	**−**	−	−	−	**+**	+	+	**−**	**−**	+	−	**+**	**+**	+	**+**	+
TRP	−	**+**	+	+	**−**	**+**	−	**−**	**−**	+	−	**+**	−	**+**	+	+	+	−	−	**+**	+	+	+	−
TRF	+	+	+	−	+	+	**+**	−	−	**+**	+	−	+	**+**	+	+	−	+	+	**+**	**+**	−	+	−
KDZ	+	**+**	+	−	−	+	**+**	+	**−**	**+**	+	**+**	−	**+**	**−**	−	+	+	−	**+**	**+**	−	−	−
OLT	−	+	+	+	−	+	**+**	−	−	**+**	**+**	+	−	−	+	−	−	**−**	+	**+**	**+**	**+**	+	**−**

Figure 3. Climate response functions summarized as positive and negative response function elements. Bold + signs indicate positive significant elements, light + signs other positive elements. Bold—signs indicate significant negative elements, light—signs other negative elements, where $p \leq 0.05$. Site codes are those used in Table 1 and Figure 1. Statistics of these response functions are given in Table 1.

SIGNATURE YEARS

Signature years were then examined (Huber and Giertz 1970; Schweingruber *et al.* 1990). A year's signature is the sign of the difference between that year's ring-width index and that of the previous year. We defined a regional signature year as one in which at least 18 out of the 23 chronologies (approximately 78%) have the same sign. Fourteen positive and twelve negative regional signature years are present in the analysis period (Table 2). Using a Monte Carlo simulation based on 10,000 replications, we determined that 23 random 100-year long time series would have less than one-tenth this number of signature years (0.88 positive signature years and 0.76 negative).

CLIMATE IN SIGNATURE YEARS

The April–June precipitation of the eastern Mediterranean region differed in the regional signature years as compared with non-signature years. The mean deviation in precipitation for the 14 positive signature years is consistently positive and the mean deviation for the 12 negative signature years is consistently negative from western Greece to the Caucasus as shown in composite maps of anomalies (Figures 4a and 4b). A composite is simply an average of the data at each grid point for which data are available. In this case a 2.5° latitude by 2.5° longitude grid of precipitation anomalies was calculated for the region bounded by 50°N–30°N and 5°E–50°E. Station data from Eischeid *et al.* 1991 were used for this. Climatic data are often expressed as anomalies, that is departures from some long-term mean, in this case 1921–1990. Thus, the positive signature years' precipitation composite (Figure 4a) was constructed by calculating the average precipitation anomaly at each gridpoint for the years 1930, 1933, 1936, 1959, 1960, and 1975. The statistical significance of the mean anomaly for each gridpoint was assessed using Student's t-test. Because an F-test indicated that both the overall population and the composite sample have equal variances, the variance in Student's t-test is the pooled variance of the two data sets. Evaluation of the significance of the difference between the two means was done by determining the probability of getting a difference (i.e. a composite anomaly) as large or larger than the difference exhibited, given the size of the samples. In the significance test we conducted, the degrees of freedom equaled the number of years

Table 2. Years in which 18 or more of the 23 tree-ring chronologies showed a change in the same direction (see text for explanation).

Increase	Decrease
1881	1882
1895	1886
1896	1887
1897	1890
1901	1916
1910	1918
1917	1928
1919	1935
1930	1942
1933	1945
1936	1949
1959	1961
1960	
1975	

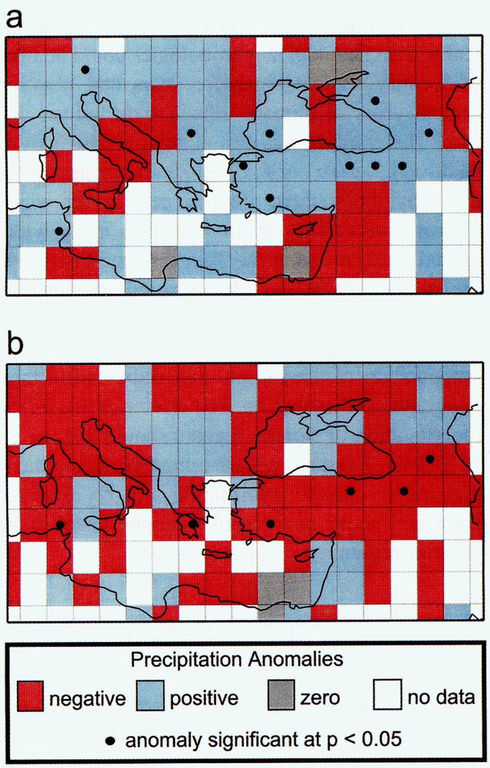

Figure 4. a. Composite of total April through June precipitation for the positive signature years. b. Composite of total April through June precipitation for the negative signature years.

in the composite plus the number of years with which it is being compared minus 2.

Charts of sea level pressure (SLP), calculated as anomalies from the long-term mean (1921–1990) for each gridpoint, provide insights to some aspects of atmospheric circulation. In this case the data used were monthly sea level pressure (in millibars, mb) on a 5° by 5° grid from 85°N–15°N. The data were in the form of anomalies from the mean for 1951–1980. Figures 5a and 5b show composite maps of mean SLP anomalies during the April–June period for the 14 positive and 12 negative signature years. The most striking feature of the positive years' map is a positive anomaly at high latitude, interpreted as a tendency for a blocking high to develop in the Arctic, associated with an expansion of the circumpolar jet, strongly

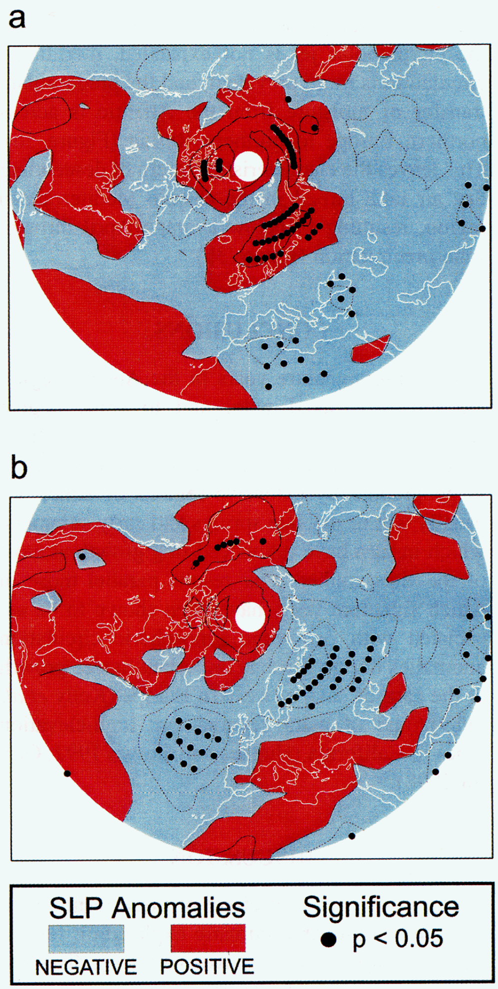

Figure 5. a. Composite of April through June sea level pressure (SLP) anomalies for the positive signature years. b. Composite of April through June sea level pressure anomalies for the negative signature years. See text for explanation of the terms 'composite' and 'anomaly.' Red areas indicate positive anomalies (higher SLP than the mean) and the blue shaded area negative anomalies (lower SLP). The anomalies are contoured at 0.5 mb intervals (continuous and dashed black lines).

zonal circulation, and a southerly displacement of storm tracks. These bring an unusually large amount of precipitation to the eastern Mediterranean region in April–June, as illustrated in Figures 5a and 4a. Conversely, the negative signature years are associated with a circulation pattern in which the high latitude blocking high does not develop, the circumpolar jet is not expanded, meridional circulation is more prevalent, and the predominant transfer of moisture from the Atlantic is across northern Europe to northern Russia (Figure 5b). This leaves the characteristic pattern of descending dry air undisturbed in the eastern Mediterranean region, resulting in below average April through June precipitation (Figure 3b).

CONCLUSIONS

Tree-ring signature years in the Aegean region are thus associated with, and to some degree caused by, persistent seasonal patterns of atmospheric circulation. These particular patterns result in geographically extensive regions of either unusually wet or dry late springs and early summers, which in turn have influenced ring growth at most of the sites studied. Our results parallel those in which signature years have been shown to be associated with persistent atmospheric circulation anomalies during seasons important to tree growth in the case of oaks in western Europe (Kelly *et al.* 1989), and of giant sequoia and high-elevation pines in California (Hughes and Brown 1992; Garfin 1998).

DISCUSSION

The most important effect of these results is to provide a reasonable climatic explanation for the existence of cross-dating over very long distances in these regions. Dendrochronologists may well make the assumption that long-distance crossdating is explained by the impact of consistent large-scale circulation features on the climate elements that influence ring growth. Here we provide an objective basis for accepting this assumption.

This opens up tantalizing possibilities for future dendroclimatological research in this region for any time period before weather records are available that is covered by well-replicated tree-ring chronologies: that is to say, most of the last 5,000 years and about half of the preceding four millennia. The fact that this is such a large-scale phenomenon allows for the precise provenance of the trees to be unimportant, at least in signature years, as noted by Kelly *et al.* (1989). Therefore historical and archaeological chronologies could be used to identify ancient signature years and possibly critical years of climate influence on human history. There are, however, a number of issues to be dealt with before our findings should be applied in this way. First, there are few periods for which tree-ring material is available for as many widespread locations as in the 20th century. Therefore, the robustness of the identification of signature years in smaller datasets should be examined. Second, there are long-term shifts in the tree species composition of the sample materials, and in their geographical distribution. The effects of this on the identification of signature years should also be investigated. Even so, we are optimistic that reliable and useful climate information will be extracted from the record of regional signature years in the Aegean region.

REFERENCES CITED

Cook, E. R.
1985 *A Time Series Approach to Tree-Ring Standardization.* Ph.D. dissertation, University of Arizona. Tucson.

Douglass, A. E
1914 A method of estimating rainfall by the growth of trees. In *The Climatic Factor,* edited by E. Huntington, pp. 101–122. Carnegie Institution of Washington Publication 289.

Eischeid, J. K., H. F. Diaz, R. S. Bradley, and P. D. Jones
1991 *A Comprehensive Precipitation Data Set for Global Land Areas.* US Department of Energy Technical Report Number TR051. US Department of Energy, Carbon Dioxide Research Program; 82 pp.

Fritts, H. C., T. J. Blasing, B. P. Hayden, and J. E. Kutzbach
1971 Multivariate techniques for specifying tree-growth and climate relationships and for reconstructing anomalies in climate. *Journal of Applied Meteorology* 10(5):845–864.

Garfin, G. M.
1998 Relationships between winter atmospheric circulation patterns and extreme tree growth anomalies in the Sierra Nevada. *International Journal of Climatology* 1:725–740.

Gassner, G., and F. Christiansen-Weniger
1942 Dendroklimatologische Untersuchungen über die Jahresringentwicklung der Kiefern in Anatolien. *Nova Acta Leopoldina: Abhandlungen der Kaiserlich Leopoldinisch-Carolinisch deutschen Akademie der Naturforscher N.F.,* Band 12, Nr. 80.

Huber, B., and V. Giertz
1970 Central European dendrochronology for the Middle Ages. In *Scientific Methods in Medieval Archaeology*, edited by R. Berger.

Hughes, M. K, and P. M. Brown
1992 Drought frequency in central California since 101 B.C. recorded in giant sequoia tree rings. *Climate Dynamics* 6:161–167.

Kelly, P. M., M. A. R. Munro, M. K. Hughes, and C. M. Goodess
1989 Climate and signature years in West European Oaks. *Nature, London* 340:57–60.

Kuniholm, P. I.
1990 The archaeological record: evidence and non-evidence for climatic change. In *The Earth's Climate and Variability of the Sun Over Recent Millennia*, edited by S. K. Runcorn and J.-C. Pecker, pp. 645–655. Phil. Trans. R. Soc. Lond. A.
1993 A date-list for Bronze Age and Iron Age monuments based on combined dendrochronological and radiocarbon evidence. In *Studies in Honor of Nimet Özgüç* [*Ankara: Türk Tarih Kurumu Basımevi.*], pp. 371–373.
1996 Long tree-ring chronologies for the Eastern Mediterranean. In *Archaeometry 94*, edited by S. Demirci, A. M. Özer, and G. D. Summers, pp. 401–409. Tübitak, Ankara.

Kuniholm, P. I., and M. W. Newton
1990 A 677 year long tree-ring chronology for the Middle Bronze Age. In *Studies in Honor of Tahsin Özgüç* [*Ankara: Türk Tarih Kurumu Basımevi.*]; pp. 279–293.

Kuniholm, P. I., and C. L. Striker
1987 Dendrochronological investigations in the Aegean and neighboring regions, 1983–1986. *Journal of Field Archaeology* 14:385–398.

Kuniholm, P. I., S. L. Tarter, M. W. Newton, and C. B. Griggs
1992 Dendrochronological investigations at Porsuk/Ulukışla, Turkey 1987–1989. *Syria* 1992(3/4):379–389.

Kuniholm, P. I., S. L. Tarter, and C. B. Griggs
1993 Dendrochronology Report. In *Tille Höyük 4: The Late Bronze Age and the Iron Age Transition*, edited by G. Summers, pp. 179–189. British Institute of Archaeology at Ankara.

Kuniholm, P. I., C. B. Griggs, S. L. Tarter, H. E. Kuniholm, and M. I. Pezzo
1995 A 513-Year *Buxus* chronology for the Roman Ship at Comacchio (Ferrara). *Bolletino di Archeologia.* 291.

Potter, K. W.
1981 Illustration of a new test for detecting a shift in mean precipitation series. *Monthly Weather Review* 109: 2040–2045.

Schweingruber, F. H., D. Eckstein, F. Serre-Bachet, and O. U. Bräker
1990 Identification, presentation and interpretation of event years and pointer years in dendrochronology. *Dendrochronologia* 8:9–38.

Received 6/16/00; accepted 2/5/01.